Origin of Interfacial Orbital Reconstruction in Perovskite Superlattices

Wenbo Yang,[1,2,*] Yu Ni,[1,2,*] Yingkai Liu,[1,2] Xiaobo Feng,[1,2] Jiangping Hu,[3] Wu-Ming Liu,[3,†] Ruqian Wu,[4,‡] and Zhaoming Fu[1,2,§]

[1]College of Physics and Electronic Information, Yunnan Normal University, Kunming 650500, China
[2]Yunnan Key Laboratory of Opto-Electronic Information Technology, Kunming 650500, China
[3]Beijing National Laboratory for Condensed Matter Physics, Institute of Physics, Chinese Academy of Sciences, Beijing 100190, China
[4]Department of Physics and Astronomy, University of California, Irvine, California 92697-4575, USA

(Received 5 January 2023; revised 1 February 2024; accepted 27 February 2024; published 18 March 2024)

The competition between on-site electronic correlation and local crystal field stands out as a captivating topic in research. However, its physical ramifications often get overshadowed by influences of strong periodic potential and orbital hybridization. The present study reveals this competition may become more pronounced or even dominant in two-dimensional systems, driven by the combined effects of dimensional confinement and orbital anisotropy. This leads to electronic orbital reconstruction in certain perovskite superlattices or thin films. To explore the emerging physics, we investigate the interfacial orbital disorder-order transition with an effective Hamiltonian and how to modulate this transition through strains.

DOI: 10.1103/PhysRevLett.132.126201

The electronic correlation (EC) effect in solids can give rise to complex physical phenomena and has been a subject of interdisciplinary research for decades. For example, the competition between on-site electronic correlation and periodic lattice field is the driving force for the classical metal-nonmetal Mott transition [see Fig. 1(a)]. However, little attention has been paid to the electronic phase transition caused by the competition between on-site correlation and local crystal field (EC CF competition). A possible reason is that the effect of local crystal field is always mixed with those of periodic potential and orbital hybridization in solids. As a result, it is difficult to single out the local field effect to some extent from the band structure and measurable electronic properties. In this study, we find a way to discern the effect of EC CF competition in perovskite superlattices or films and establish quantifiable criteria for typical phase transitions. This becomes possible as the periodic structures in superlattices or thin films are disrupted along the growth direction, leading to a weakened periodic modulation on the local crystal field. Obviously, this physical analysis is applicable to other low dimensional systems, and the insights drawn hold broad significance.

We take titanate superlattices with the crystal field of TiO_6 octahedrons as examples [see Fig. 1(b)], which are known for the emergence of two-dimensional electron–hole gas (2DEG/2DHG) at the interface of two insulators [1–10], such as $LaAlO_3/SrTiO_3$ (LAO/STO) [1–3]. Numerous studies have observed an unusual crystal-field splitting or reconstruction of t_{2g} orbitals at $LaAlO_3/SrTiO_3$ interfaces [11–15] as well as in the $CaVO_3$ thin film and superlattices [16,17]. Specifically, the observed electronic orbital occupations appear to challenge the conventional crystal-field theory. Yet, the physical basis of this atypical behavior remains as a long-standing mystery. Conversely, nickelate superlattices with the crystal field of NiO_6 octahedrons attract research interest due to the predictions surrounding potential Ni-based superconductivity [see Fig. 1(b)] [18–25]. Recent theoretical simulations suggest that, in the superlattice with a nickelate monolayer, an unusual crystal-field effect is present. Electrons have a strong preference to take the planar $d_{x2\text{-}y2}$ orbital, even in the absence of crystal-field splitting [26]. This indicates an unusual reconstruction that goes beyond what conventional crystal field theory predicts and highlights the possible impact of EC CF competition.

To understand emergent physics, we use density functional theory (DFT) calculations and model simulations to examine the cooperative effects of dimensional confinement

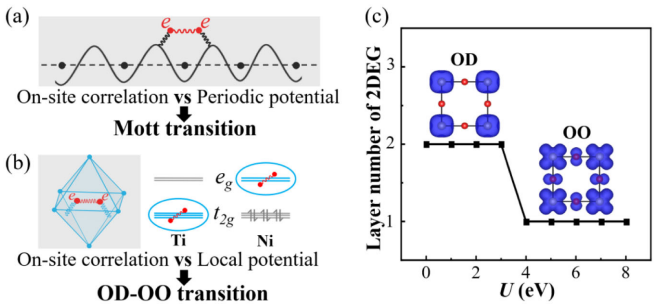

FIG. 1. (a) Sketch of competition between electronic correlation and global periodic field. (b) Sketch of competition between electronic correlation and local crystal field. (c) Layer number of 2DEG vs Hubbard U in LAO/STO from first-principle calculations. The blue insets are electron cloudy of 2DEGs with $U \leq 3$ (left) and $U > 3$ eV (right).

and anisotropic spatial orientations of d orbitals in superlattices. The former disrupts the periodic modulation and limits the electronic hopping along the growth direction, while the latter leads to the inequivalence between in-plane and out-plane orbitals [27,28]. Consequently, a phase transition from orbital disorder (OD) to orbital order (OO) occurs along with the orbital reconstruction [see Figs. 1(b) and 1(c)]. The presence of OO in perovskite bulks has attracted extensive attention [29–32], which often induces other phase transitions [33]. For details of DFT calculations and superlattice modeling, please consult Supplemental Material [34].

The effect of on-site correlations on the interfacial 2DEGs is incorporated by using a large range of U values (0–8 eV) for $3d$ electrons of Ti in DFT calculations. Interestingly, the occupied orbitals of 2DEGs are changed along with the increase of U, i.e., the orbital reconstruction occurs when U is greater than a critical value U_C ($3 < U_C < 4$ eV). The insets of Figs. 1(c) show the distributions of 2DEGs in the interfacial TiO_2 layer with $U = 3$ and 6 eV, respectively. With high U, 2DEGs have a clear quatrefoil structure in the XOY plane because electrons only occupy the d_{xy} orbitals of the interfacial Ti atoms, corresponding to an OO phase. In contrast, 2DEGs have no remarkable spatial anisotropy with $U \leq 3$ eV as all three t_{2g} (d_{xy}, d_{xz}, and d_{yz}) orbitals are equally occupied, corresponding to an OD phase. Simultaneously, the thickness of 2DEGs is also changed [see Fig. 1(c) and Supplemental Material, Fig. S1 [34]]. When the U is larger than U_C, 2DEGs are mainly localized in a single TiO_2 layer at the interface. Herein, the orbital reconstruction can be hence regarded as an OD OO phase transition [see Figs. 1(b) and 1(c)]. The curves of projected density of states (PDOS) in Fig. 2(b) further validate these deductions as only the d_{xy} component is below the Fermi level for $U = 4$ eV.

Unlike in the STO bulk, the interfacial TiO_6 octahedron is elongated in the direction perpendicular to the superlattice, with a minor out-plane displacement of the Ti ion (by 0.11 Å) in the oxygen octahedron. As a result, the O_h symmetry is reduced to the C_{4v} symmetry, causing further splittings of the e_g and t_{2g} orbitals [see Fig. 2(a)]. The three t_{2g} orbitals split into a nondegenerate d_{xy} orbital and double degenerate d_{xz}/d_{yz} orbitals. According to the standard crystal-field theory, the d_{xz}/d_{yz} orbitals should have a lower energy than the d_{xy} orbital [see Fig. 2(a)], and therefore 2DEGs should mainly occupy the d_{xz}/d_{yz} orbitals instead of the d_{xy} orbital. This is indeed true when U is smaller than U_C. However, the result is opposite for large U values as only the d_{xy} orbital is occupied, corresponding to the orbital reconstruction [see Figs. 2(a) and 2(b)]. Figure 2(b) displays how the strength of the on-site correlation significantly affects the magnitude of t_{2g} orbital splitting. Additionally, there is a notable change in the electron occupation numbers on the in-plane and out-plane

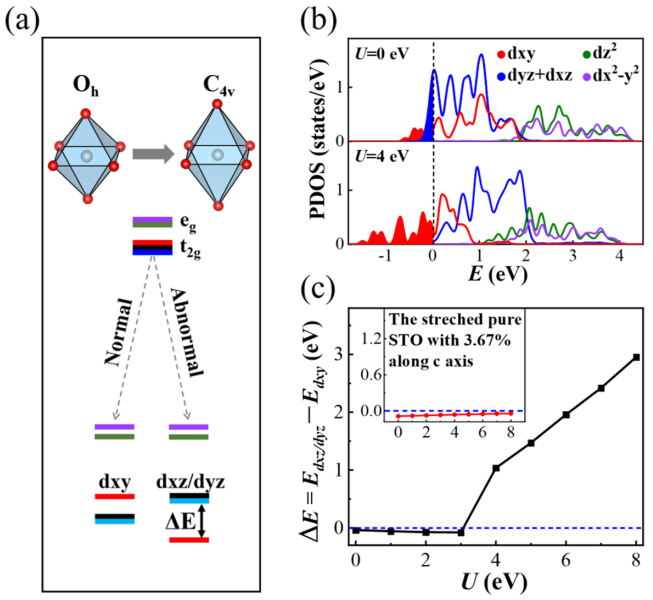

FIG. 2. (a) Distortion of interfacial TiO_6 octahedron from O_h to C_{4v} symmetry, and normal (left) and abnormal (right) d-orbital splitting of Ti. (b) First-principle calculated the projected density of states (spin up) of interfacial Ti with Hubbard $U = 0$ and 4 eV, with the filled areas representing the occupied states. (c) Splitting energy (ΔE) between d_{xy} and d_{xz}/d_{yz} vs Hubbard U from first-principle calculations. The red curve in the inset is the splitting energy vs Hubbard U for stretched STO bulk, which is simulated using a model comprised of four cubic unit cells.

orbitals [see the filled areas in Fig. 2(b)]. To clearly illustrate the splitting, we calculate the band center of each projected d orbital (E_C), from which we define the energy splitting of t_{2g} orbitals [ΔE, see Fig. 2(a)] as

$$\Delta E = E_C(d_{xz}/d_{yz}) - E_C(d_{xy}), \tag{1}$$

where E_C (d_{xz}/d_{yz}) and E_C (d_{xy}) are the band centers of d_{xz}/d_{yz} and d_{xy}, respectively. We observed that ΔE is highly sensitive to the values of Hubbard U [see Fig. 2(c)]. First, ΔE flips from negative to positive as U exceeds U_C, indicating the reversed crystal-field splitting and orbital reconstruction. The occupied states of 2DEGs change from three (d_{xy}, d_{yz}, d_{xz}) to just one (d_{xy}). Therefore, the orbital reconstruction is related to the on-site correlation of 2DEGs. Second, for small U, the splitting energy resulting from crystal-field distortion is minimal [see Fig. 2(c)]. This leads to partial electron occupation on three t_{2g} orbitals [see Fig. 2(b)], corresponding to an OD phase. However, for all U values, the energy level splitting of the e_g orbitals adheres to the crystal-field theory, as both orbitals are empty. Interestingly, the calculated magnetic phase transition has a similar critical U_C, indicating that the orbital order and magnetic order are closely related (see Fig. S2). When comparing the LAO/STO interface to the pure STO bulk, and the latter has no inversion of crystal field under

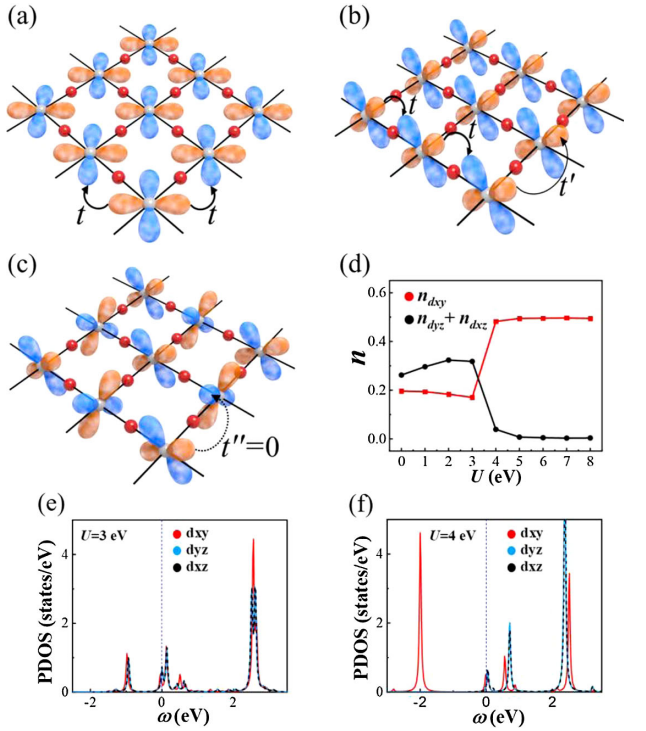

FIG. 3. (a)–(c) represent the electronic d_{xy}-d_{xy}, d_{xz}-d_{xz}, and d_{xz}-d_{yz} hopping on 2D TiO_2 lattice, respectively. $\boldsymbol{t}$ and $\boldsymbol{t}'$ represent the hopping amplitude along σ and π bonds, respectively. $\boldsymbol{t}''$ represents one between two different orbitals. (d) Electron occupation numbers on in-plane (red line) and out-plane (black line) orbitals from DMFT calculations. (e),(f) Projected density of states for the Hubbard model with $U = 3$ eV and 4 eV from DMFT calculations.

the same stretching strain [see the inset of Fig. 2(c)]. This underscores the crucial role that confinement plays. As previous work attempted to attribute the orbital reconstruction to the displacement of Ti in oxygen octahedron, we also simulate a hypothetical structure without displacement of Ti. From the results shown by Supplemental Material, Fig. S7 [34], we may see that the effect of Ti displacement is minor. Our results strongly suggest that the orbital reconstruction results from the on-site correlation and the confinement effect.

Herein, we introduce a compelling mechanism that takes into account both strong correlation and dimensionality concurrently. Because 2DEGs mainly distribute in interfacial TiO_2 layers, the dimensional confinement causes electrons to hop only in the XOY plane. As a result, the in-plane d_{xy} orbital is not equivalent to the out-plane d_{xz}/d_{yz} orbitals due to their distinct spatial orientations, as shown in Fig. 3. This is much different from the case in isotropic bulks. For Ti in the 2D TiO_2 plane, its t_{2g} orbitals can generate three different types of hopping, shown by Figs. 3(a)–3(c), respectively. The first is the hopping between in-plane d_{xy} orbitals, i.e., d_{xy}-d_{xy} hopping [see Fig. 3(a)], which has the same hopping amplitudes ($\boldsymbol{t}$) along the X and Y directions. Furthermore, adjacent d_{xy} orbitals are connected through σ bonds, and hence have a large hopping amplitude. This type of interaction is described by the isotropic 2D Hubbard model as the on-site correlation is considered. The second is the hopping between two identical out-plane orbitals, i.e., d_{xz}-d_{xz} (or d_{yz}-d_{yz}) hopping [see Fig. 3(b)], in which two neighboring d_{xz} orbitals form σ bonds along the X direction, but π bonds along the Y direction. Therefore, the hopping amplitude along the X direction is close to that of the first type ($\boldsymbol{t}$), but the hopping amplitude along the Y direction is much smaller ($\boldsymbol{t}' \ll \boldsymbol{t}$) due to less orbital overlap. This type of interaction can be described by the quasi 1D Hubbard model. The third is the hopping between two different orbitals, such as d_{xz}-d_{yz} hopping [see Fig. 3(c)], which is actually forbidden in this system due to the mirror symmetry ($\boldsymbol{t}'' = 0$, see Fig. S3). Studies of 1D and 2D Hubbard models have confirmed that, for the same parameters (hopping amplitude, U value, and chemical potential), the 2D Hubbard model has a lower ground-state energy than the 1D Hubbard model [46]. This conclusion is understandable because the higher dimension (larger ligancy) can reduce the probability of double occupation as electrons hop on lattices, and hence reduce the on-site Coulomb repulsion and ease the energy. Consequently, 2DEGs prefer to take the d_{xy} orbitals with a reversed crystal-field splitting. Based on these discussions, it is clear that the "synergy" of dimensional confinement, orbital orientation, and on-site correlation collectively contributes to making the in-plane d_{xy} orbitals energetically more favorable. According to the orbital overlap, we can also explain why the orbital reconstruction is simultaneous with the ferromagnetic phase transition. On the one hand, the in-plane d_{xy} orbitals contribute a large overlap integral of wave function along both x and y directions, corresponding to a larger exchange coupling, i.e., the orbital reconstruction would lead to a strong magnetic interaction. On the other hand, the Hubbard model can degenerate to Stoner model in the mean field approximation, which can describe the formation of ferromagnetic phase after orbital reconstruction.

To further address the effect of electron correlation, we constructed an effective Hamiltonian of three-orbital Hubbard model [Eq. (2)] based on a two-dimensional square lattice like the TiO_2 layer to describe the interfacial 2DEGs.

$$\begin{aligned} H = &-\sum_{il\sigma}\left(t_{lx}d^{+}_{il\sigma}d_{i+x,l\sigma} + t_{lx}d^{+}_{il\sigma}d_{i-x,l\sigma}\right. \\ &\left. + t_{ly}d^{+}_{il\sigma}d_{i+y,l\sigma} + t_{ly}d^{+}_{il\sigma}d_{i-y,l\sigma}\right) \\ &+ \sum_{il\sigma}(\epsilon_l - \mu)d^{+}_{il\sigma}d_{il\sigma} + \frac{U}{2}\sum_{il\sigma} n_{il\sigma}n_{il\bar{\sigma}} \\ &+ U' \sum_{i,l<l',\sigma\sigma'} n_{il\sigma}n_{il'\sigma'}. \end{aligned} \tag{2}$$

Herein, $d^{+}_{il\sigma}$ ($d_{il\sigma}$) is an electron creation (annihilation) operator for orbital l (=1, 2, and 3 for d_{xy}, d_{xz}, and d_{yz})

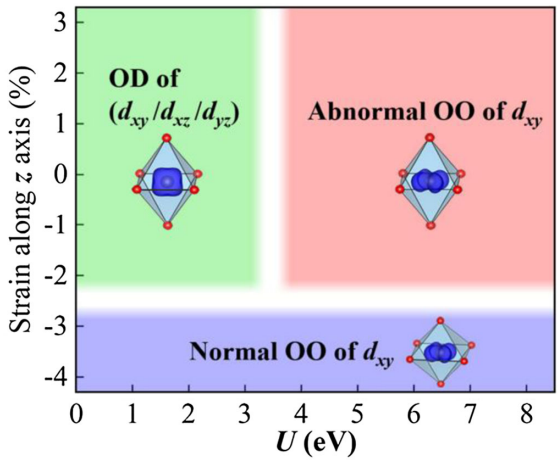

FIG. 4. Phase diagram of orbital order (OO) of interfacial 2DEGs vs Hubbard U and uniaxial straining from first-principle calculations. The insets are the spatial structures of 2DEGs under the corresponding sections of staining and U values.

at site i with spin σ. $n_{il\sigma} = d^{+}_{il\sigma} d_{il\sigma}$ represents the corresponding electron occupation and t_{lx} (t_{ly}) denotes the nearest neighbor hopping along the x direction (y direction) of orbital l. ϵ_l,μ, U, and U' represent the on-site energy of orbital l, chemical potential, intraorbital, and interorbital correlation interaction. The hopping integrals are obtained using the Wannier function downfolding technique, which strongly support the deduction on the characteristics of hopping amplitude (see Supplemental Material, Fig. S4 [34]). We calculated the electron occupation numbers on in-plane and out-plane orbitals using the dynamical mean-field theory (DMFT, see Supplemental Material [34]) [Fig. 3(d)]. A switch between occupations on in-plane and out-plane orbitals is observed along with increasing Hubbard U, with a critical U value between 3 and 4 eV. From the PDOS in Figs. 3(e) and 3(f), we found that the in-plane d_{xy} orbital (red curve) has an abrupt change in energy as the Hubbard UU increases from 3 to 4 eV. Its electron occupation number also jumps. These observations align with outcomes of first-principles calculations. Additionally, the roles of Hund coupling and features of Hamiltonian are discussed in Fig. S5 and Supplementary Material [34]. It is found that the critical U value of orbital reconstruction can be tuned by the Hund coupling strength (see Figs. S6). According to the understandings on the interfacial Hubbard interaction, the change in 2DEG's thickness for different U values, shown in Fig. S1a, can also be explained (for more information on this, please refer to Fig. S6 and corresponding discussions in Supplemental Material).

We also investigate the effect of uniaxial strain on the orbital reconstruction of 2DEGs (see Figs. 4 and S8). The uniaxial strain (κ_z) is defined as

$$\kappa_z = \frac{\boldsymbol{c}_{\text{strain}} - \boldsymbol{c}_{\text{strainless}}}{\boldsymbol{c}_{\text{strainless}}}, \tag{3}$$

where $\boldsymbol{c}_{\text{strain}}$ and $\boldsymbol{c}_{\text{strainless}}$ are lattice parameters of superlattice with and without tensile or compressive strain along the growth direction. Our result indicates that OD-OO transition can sustain under small strains. In the case of large tensile strain, the crystal field is energetically in favor of the d_{xz} and d_{yz} orbital as the interfacial TiO_6 octahedron is "elongated" along the z axis. Nevertheless, a strong on-site correlation can still lead to abnormal crystal-field splitting (abnormal OO). In contrast, large compressive strain causes a "squashed" TiO_6 octahedron along the z axis. Both crystal field and on-site correlation lower the energy of the d_{xy} orbital, and 2DEGs are in the OO phase (normal OO) even without on-site correlation.

Additionally, we also studied possible factors that may affect experimental observations on orbital reconstruction, including oxygen defects (see Fig. S9) [14], thickness of LAO and STO blocks (see Fig. S10), and orbital hybridization of Ti and O (see Fig. S11). It was found that they do not change our conclusions on orbital reconstruction of 2DEGs. Last, we postulate that the possible orbital reconstruction in nickelate superlattice with a nickelate monolayer has a similar physical mechanism, but the orbital reconstruction occurs for the $e_g d$ orbitals. In summary, we found that the competition between the on-site correlation and local crystal field is enhanced at interfaces of some superlattice systems by the dimensional confinement. Different spatial orientations make orbitals nonequivalent in local crystal field and give varying hopping amplitudes. Importantly, these intricate interplays drive orbital reconstruction and yield observable electronic phase transition.

We thank Professor Yongzhong Chen at Beijing National Laboratory for Condensed Matter Physics for valuable discussion. This work was supported by the National Natural Science Foundation of China (Grants No. 12264055, No. 12264056, No. 12264057, No. 61835013, No. 12234012) and National Key R&D Program of China (Grants No. 2021YFA1400900, No. 2021YFA0718300, No. 2021YFA1402100). Work at U. C. I. was supported by the U.S. Department of Energy, Office of Science, Basic Energy Sciences, under Award No. DE-FG02-05ER46237.

*These authors contributed equally to this work.
†wmliu@iphy.ac.cn
‡wur@uci.edu
§fuzhm1979@163.com

[1] F. Zhang *et al.*, Phys. Rev. Lett. **122**, 257601 (2019).
[2] A. Ohtomo and H. Y. Hwang, Nature (London) **427**, 423 (2004).
[3] H. Lee *et al.*, Nat. Mater. **17**, 231 (2018).
[4] J. Betancourt, T. R. Paudel, E. Y. Tsymbal, and J. P. Velev, Phys. Rev. B **96**, 045113 (2017).
[5] T. R. Paudel and E. Y. Tsymbal, Phys. Rev. B **96**, 245423 (2017).
[6] P. Xu *et al.*, Adv. Mater. **29**, 1604447 (2017).

[7] C. Bhandari and S. Satpathy, Phys. Rev. B **98**, 041303 (2018).
[8] W. Aggoune and C. Draxl, npj Comput. Mater. **7**, 174 (2021).
[9] I. V. Maznichenko, P. Buczek, I. Mertig, and S. Ostanin, Phys. Rev. Mater. **6**, 064001 (2022).
[10] M. Trama, V. Cataudella, C. A. Perroni, F. Romeo, and R. Citro, Nanomater. Nanotechnol. **13**, 819 (2023).
[11] M. Salluzzo *et al.*, Phys. Rev. Lett. **102**, 166804 (2009).
[12] P. Delugas, A. Filippetti, V. Fiorentini, D. I. Bilc, D. Fontaine, and P. Ghosez, Phys. Rev. Lett. **106**, 166807 (2011).
[13] J. S. Lee, Y. W. Xie, H. K. Sato, C. Bell, Y. Hikita, H. Y. Hwang, and C. C. Kao, Nat. Mater. **12**, 703 (2013).
[14] A. Chikina, F. Lechermann, M.-A. Husanu, M. Caputo, C. Cancellieri, X. Wang, T. Schmitt, M. Radovic, and V. N. Strocov, ACS Nano **12**, 7927 (2018).
[15] R. J. Green *et al.*, Phys. Rev. Mater. **5**, 065004 (2021).
[16] S. Beck, G. Sclauzero, U. Chopra, and C. Ederer, Phys. Rev. B **97**, 075107 (2018).
[17] S. Beck and C. Ederer, Phys. Rev. Mater. **4**, 125002 (2020).
[18] J. Chaloupka and G. Khaliullin, Phys. Rev. Lett. **100**, 016404 (2008).
[19] P. Hansmann, X. Yang, A. Toschi, G. Khaliullin, O. K. Andersen, and K. Held, Phys. Rev. Lett. **103**, 016401 (2009).
[20] A. S. Botana and M. R. Norman, Phys. Rev. X **10**, 011024 (2020).
[21] X. Wu, D. Di Sante, T. Schwemmer, W. Hanke, H. Y. Hwang, S. Raghu, and R. Thomale, Phys. Rev. B **101**, 060504 (2020).
[22] P. Adhikary, S. Bandyopadhyay, T. Das, I. Dasgupta, and T. Saha-Dasgupta, Phys. Rev. B **102**, 100501 (2020).
[23] D. Li, K. Lee, B. Y. Wang, M. Osada, S. Crossley, H. R. Lee, Y. Cui, Y. Hikita, and H. Y. Hwang, Nature (London) **572**, 624 (2019).
[24] J. Zhang, A. S. Botana, J. W. Freeland, D. Phelan, H. Zheng, V. Pardo, M. R. Norman, and J. F. Mitchell, Nat. Phys. **13**, 864 (2017).
[25] J. Karp, A. Hampel, and A. J. Millis, Phys. Rev. B **105**, 205131 (2022).
[26] R. Chavez Zavaleta, S. Fomichev, G. Khaliullin, and M. Berciu, Phys. Rev. B **104**, 205111 (2021).
[27] Z. Fu, B. Yang, and R. Wu, Phys. Rev. Lett. **125**, 156001 (2020).
[28] Z. Fu, M. Liu, and Z. Yang, Phys. Rev. B **99**, 205425 (2019).
[29] H. Yang *et al.*, Phys. Rev. B **91**, 174405 (2015).
[30] S. Lee *et al.*, Phys. Rev. Lett. **123**, 117201 (2019).
[31] A. T. Lee and C. A. Marianetti, Phys. Rev. B **97**, 045102 (2018).
[32] R. Cong, R. Nanguneri, B. Rubenstein, and V. F. Mitrović, Phys. Rev. B **100**, 245141 (2019).
[33] C. Svoboda, W. Zhang, M. Randeria, and N. Trivedi, Phys. Rev. B **104**, 024437 (2021).
[34] See Supplemental Material at http://link.aps.org/supplemental/10.1103/PhysRevLett.132.126201 for more details of methods and more results, which includes Refs. [35–45].
[35] G. Kresse and J. Furthmüller, Comput. Mater. Sci. **6**, 15 (1996).
[36] P. E. Blöchl, Phys. Rev. B **50**, 17953 (1994).
[37] G. Kresse and D. Joubert, Phys. Rev. B **59**, 1758 (1999).
[38] J. P. Perdew, K. Burke, and M. Ernzerhof, Phys. Rev. Lett. **77**, 3865 (1996).
[39] N. Nakagawa, H. Y. Hwang, and D. A. Muller, Nat. Mater. **5**, 204 (2006).
[40] N. Marzari and D. Vanderbilt, Phys. Rev. B **56**, 12847 (1997).
[41] I. Souza, N. Marzari, and D. Vanderbilt, Phys. Rev. B **65**, 035109 (2001).
[42] A. A. Mostofi, J. R. Yates, G. Pizzi, Y.-S. Lee, I. Souza, D. Vanderbilt, and N. Marzari, Comput. Phys. Commun. **185**, 2309 (2014).
[43] G. Pizzi *et al.*, J. Phys. Condens. Matter **32**, 165902 (2020).
[44] A. Koga, N. Kawakami, T. M. Rice, and M. Sigrist, Phys. Rev. Lett. **92**, 216402 (2004).
[45] R. Arita and K. Held, Phys. Rev. B **72**, 201102 (2005).
[46] T.-H. Lee, T. Ayral, Y.-X. Yao, N. Lanata, and G. Kotliar, Phys. Rev. B **99**, 115129 (2019).